

OVERFLOW Analysis of Supersonic Retropropulsion Testing on the CobraMRV Mars Entry Vehicle Concept

K. V. Matsuno¹, R. E. Childs², T. H. Pulliam², P. M. Stremel² & J. A. Garcia¹

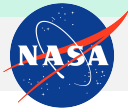


NASA Ames Research Center, Moffett Field, California 94305

¹ *NASA Systems Analysis Office*

² *Science & Technology Corporation*

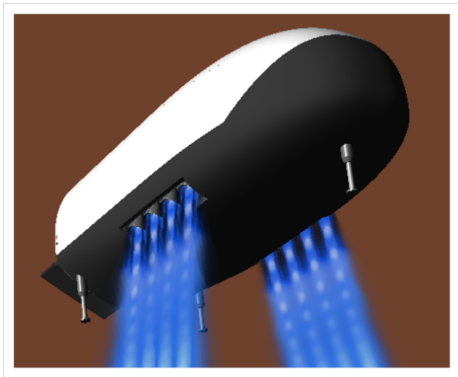
2022 AIAA SciTech Forum



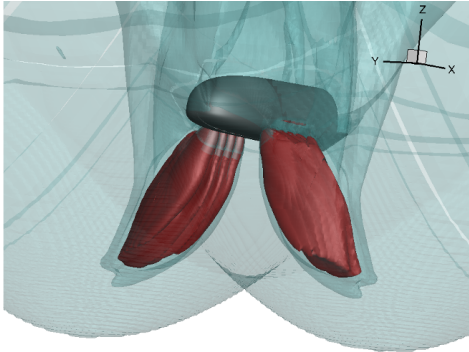
Background: CobraMRV

The CobraMRV considered for landing large payloads:

Artistic render



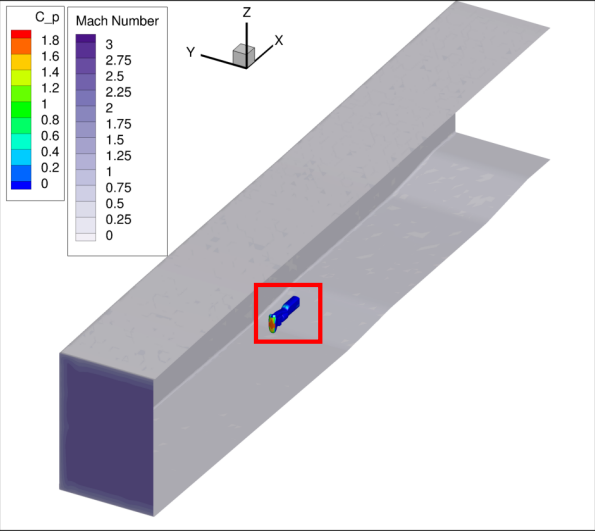
Mach number isosurfaces





Background: Tunnel & Model Geometry

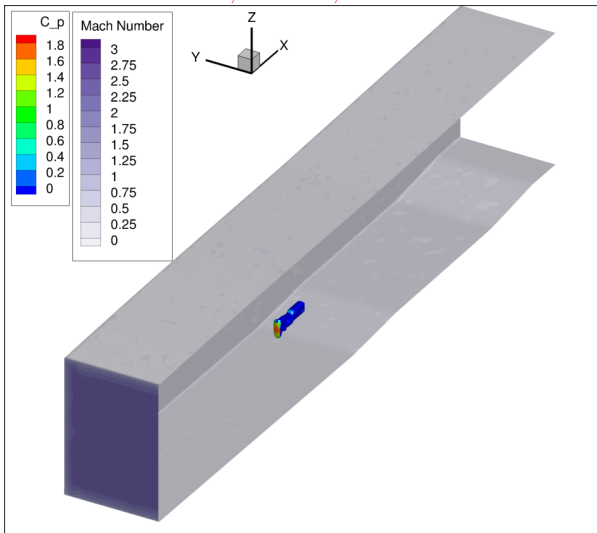
$$M = 2.4, \alpha = 90^\circ, CT = 2.5$$



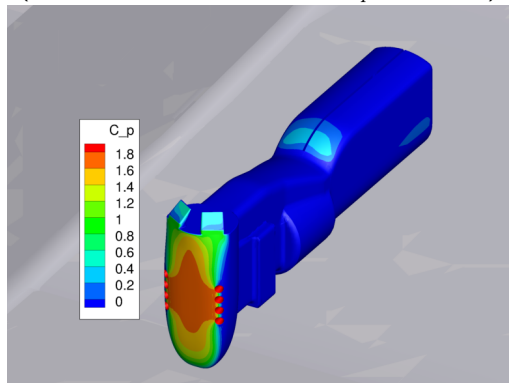


Background: Tunnel & Model Geometry

$$M = 2.4, \alpha = 90^\circ, CT = 2.5$$

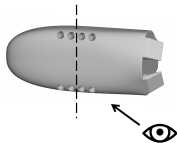


Close up view of the model & sting
(heatshield highlighted by C_p contours)





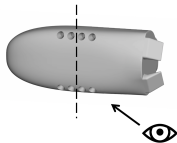
Background: Flow field visualization



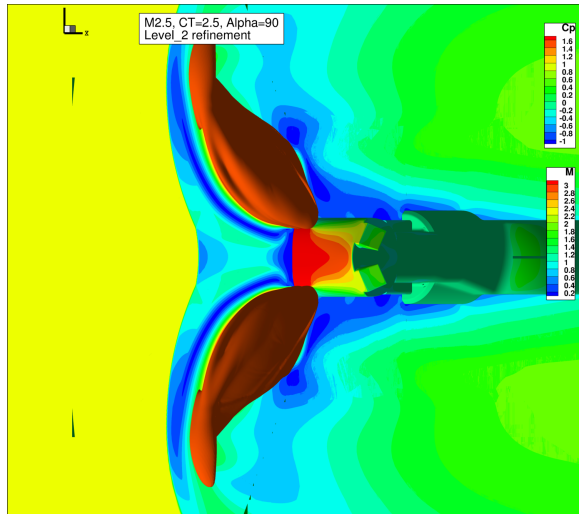
- $M = 2.386$, $\alpha = 90^\circ$ and $CT = 2.5$
- T_0 isosurfaces showing plume structures



Background: Flow field visualization

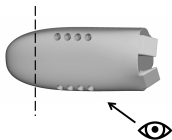


- $M = 2.386$, $\alpha = 90^\circ$ and $CT = 2.5$
- T_0 isosurfaces showing plume structures

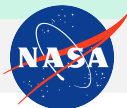




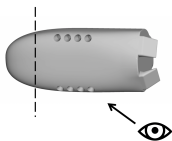
Background: Flow field visualization



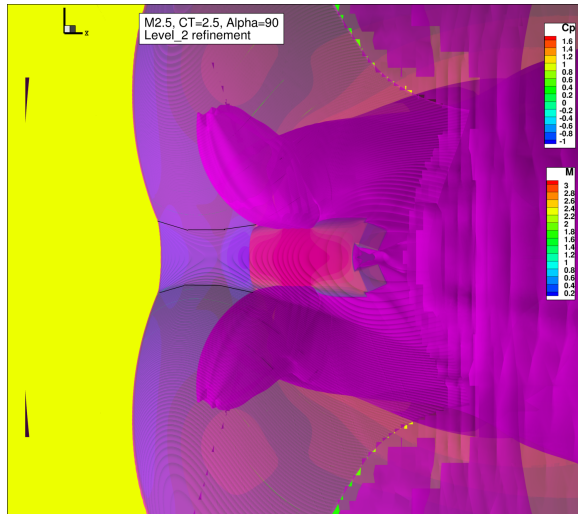
- $M = 2.386$, $\alpha = 90^\circ$ and $CT = 2.5$:
- Mach number isosurfaces
- Black lines indicating the 'saddle' shock
- Bow shock changes load dynamics



Background: Flow field visualization



- $M = 2.386$, $\alpha = 90^\circ$ and $CT = 2.5$:
- Mach number isosurfaces
- Black lines indicating the 'saddle' shock
- Bow shock changes load dynamics





Background: Heatshield

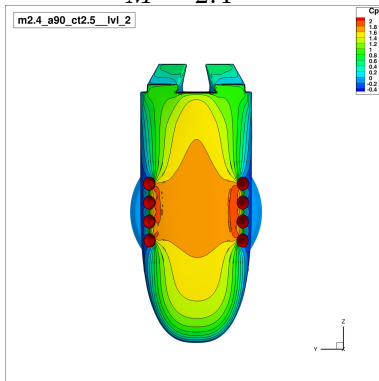
Steady C_p distributions on the heatshield at $\alpha = 90^\circ$ and $CT = 2.5$:



Background: Heatshield

Steady C_p distributions on the heatshield at $\alpha = 90^\circ$ and $CT = 2.5$:

$M = 2.4$

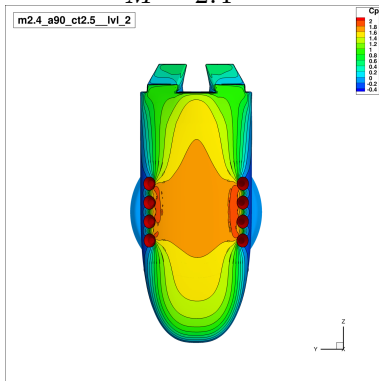




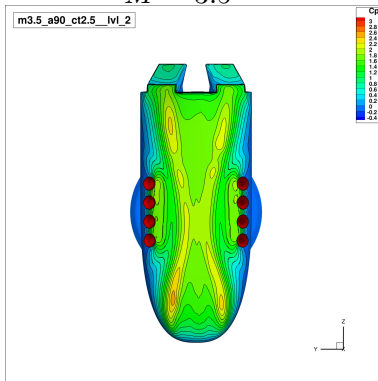
Background: Heatshield

Steady C_p distributions on the heatshield at $\alpha = 90^\circ$ and $CT = 2.5$:

$M = 2.4$



$M = 3.5$

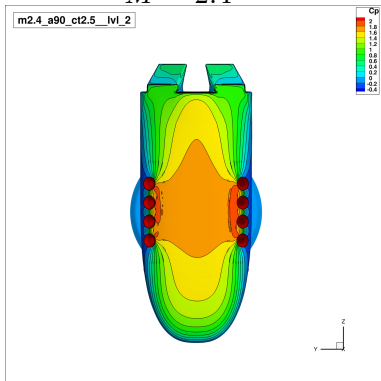




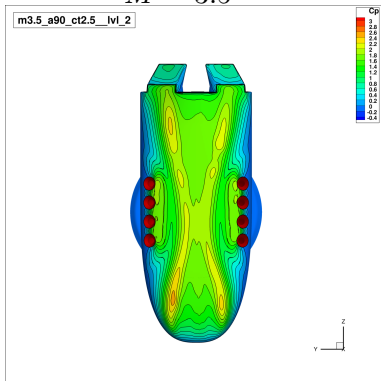
Background: Heatshield

Steady C_p distributions on the heatshield at $\alpha = 90^\circ$ and $CT = 2.5$:

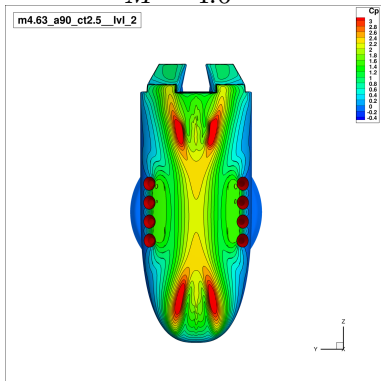
$M = 2.4$



$M = 3.5$



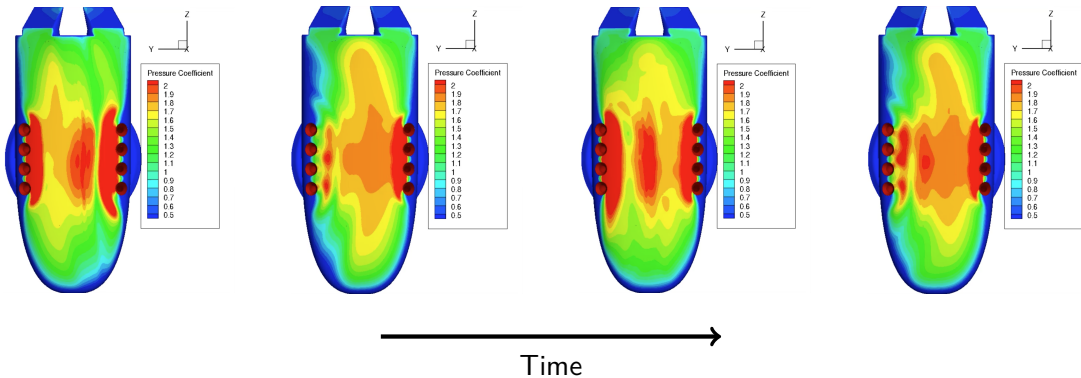
$M = 4.6$





Background: Heatshield

$M = 4.6, \alpha = 90^\circ$ and $CT = 1.0$:
An example of flow unsteadiness in heatshield C_p





Objectives

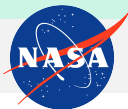
- Highlight CobraMRV SRP flow characteristics*
- Summarize CobraMRV aerodynamics*
- Investigate vehicle loads' sensitivity to CFD parameters



Objectives

- Highlight CobraMRV SRP flow characteristics*
- Summarize CobraMRV aerodynamics*
- Investigate vehicle loads' sensitivity to CFD parameters
 - Shock capturing*
 - Temporal accuracy
 - Adaptive mesh refinement (AMR)
 - Tunnel inflow conditions
 - URANS vs. DES

*See paper more detailed discussion



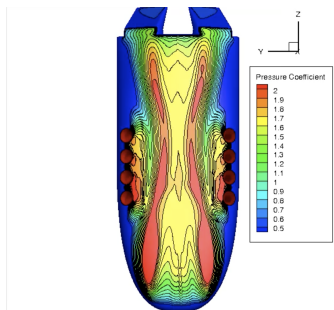
Objectives

- Highlight CobraMRV SRP flow characteristics*
- Summarize CobraMRV aerodynamics*
- Investigate vehicle loads' sensitivity to CFD parameters
 - Shock capturing*
 - Temporal accuracy
 - Adaptive mesh refinement (AMR)
 - Tunnel inflow conditions
 - URANS vs. DES

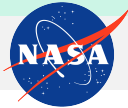
*See paper more detailed discussion

Operating conditions of particular interest:

$$M = 3.5, \alpha = 85^\circ, CT = 2.5$$



Shown: transition from 1 to 2 levels of AMR



Temporal Accuracy

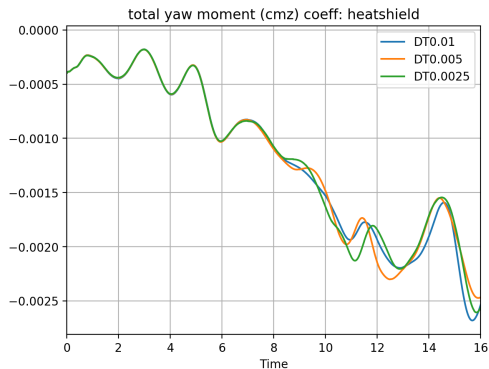
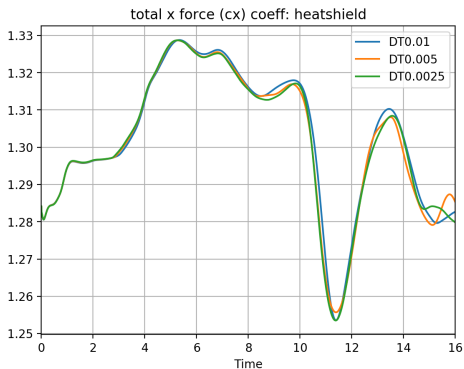
- $M = 3.5, \alpha = 85^\circ, CT = 2.5$
- What contributes to load unsteadiness, if it exists?

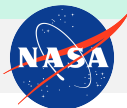


Temporal Accuracy: Δt

$$M = 3.5, \alpha = 85^\circ, CT = 2.5$$

Time-step size was not a factor in observed unsteadiness.

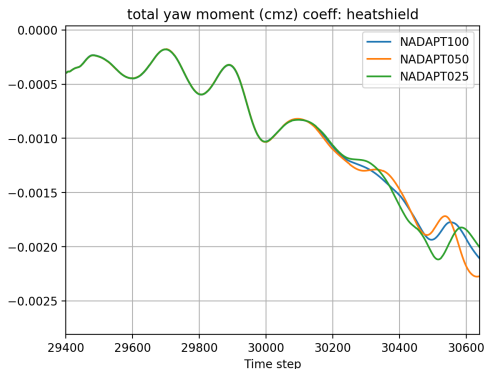
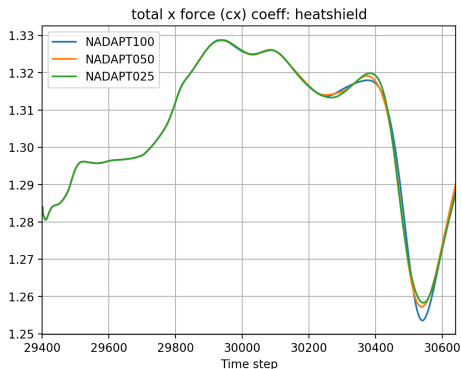




Temporal Accuracy: AMR

$$M = 3.5, \alpha = 85^\circ, CT = 2.5$$

Mesh adaption frequency was not a factor in observed unsteadiness.

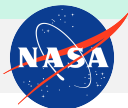




Temporal Accuracy: AMR

$$M = 3.5, \alpha = 85^\circ, CT = 2.5$$

Effect of mesh adaption frequency on heatshield loads: **Dynamic** vs. 'frozen' grid adaption

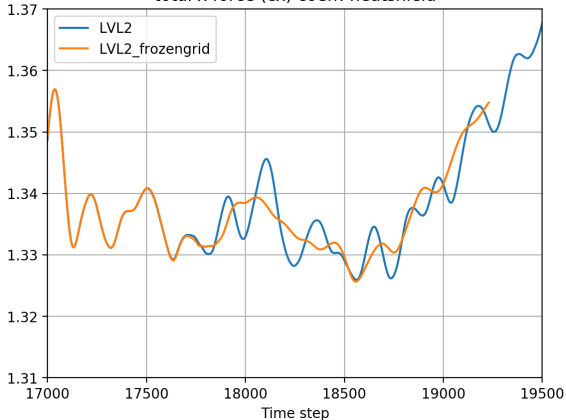


Temporal Accuracy: AMR

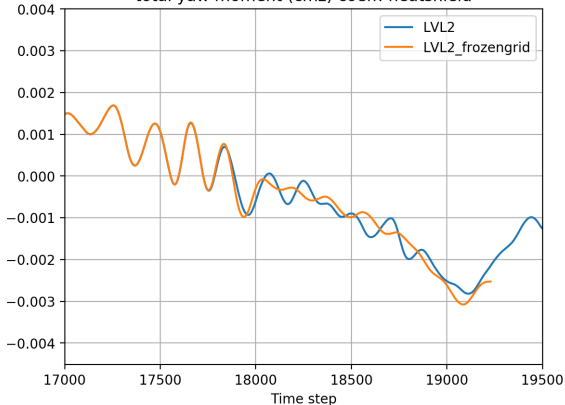
$$M = 3.5, \alpha = 85^\circ, CT = 2.5$$

Effect of mesh adaption frequency on heatshield loads: **Dynamic** vs. 'frozen' grid adaption

total x force (cx) coeff: heatshield



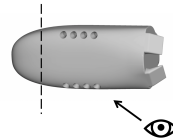
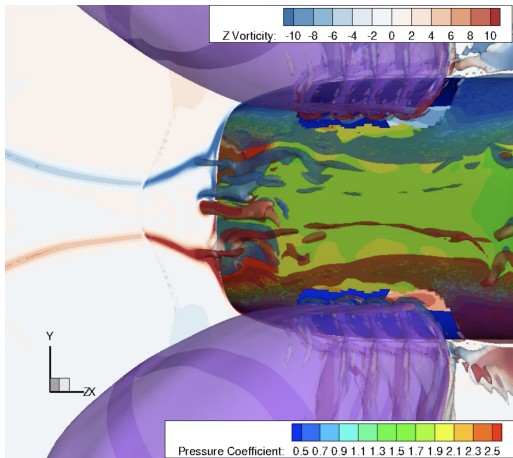
total yaw moment (cmz) coeff: heatshield



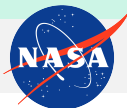


Temporal Accuracy: AMR

$$M = 3.5, \alpha = 85^\circ, CT = 2.5$$



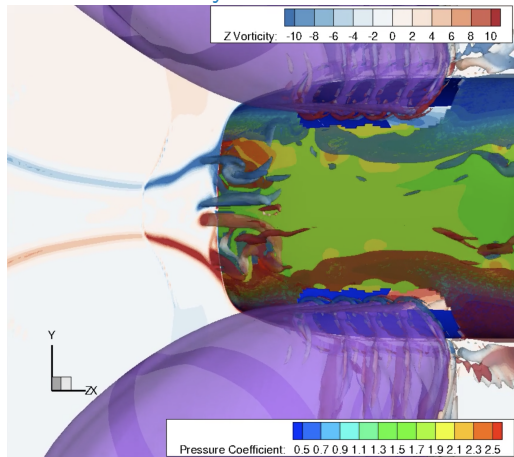
Dynamic grid adaption captures near-surface vortical structures as they travel.



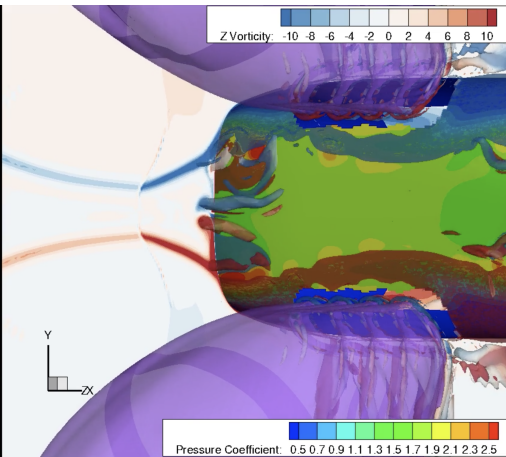
Temporal Accuracy: AMR

$$M = 3.5, \alpha = 85^\circ, CT = 2.5$$

Dynamic AMR



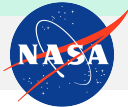
Frozen AMR





Inflow BC

¹Childs et al. "Flow Characterization of the NASA Langley Unitary Plan Wind Tunnel, Test Section 2: Computational Results," AIAA Aviation (2021)



Inflow BC

- Wind tunnel upstream of the test section has physical asymmetry

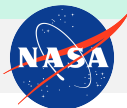
¹Childs et al. "Flow Characterization of the NASA Langley Unitary Plan Wind Tunnel, Test Section 2: Computational Results," AIAA Aviation (2021)



Inflow BC

- Wind tunnel upstream of the test section has physical asymmetry
- Test section inflow BC from empty tunnel CFD¹

¹Childs et al. "Flow Characterization of the NASA Langley Unitary Plan Wind Tunnel, Test Section 2: Computational Results," AIAA Aviation (2021)



Inflow BC

- Wind tunnel upstream of the test section has physical asymmetry
- Test section inflow BC from empty tunnel CFD¹
- Does inflow BC asymmetry propagate to heatshield loads?

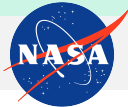
¹Childs et al. "Flow Characterization of the NASA Langley Unitary Plan Wind Tunnel, Test Section 2: Computational Results," AIAA Aviation (2021)



Inflow BC

- Wind tunnel upstream of the test section has physical asymmetry
- Test section inflow BC from empty tunnel CFD¹
- Does inflow BC asymmetry propagate to heatshield loads?
- $M = 3.5, \alpha = 85^\circ, CT = 2.5$

¹Childs et al. "Flow Characterization of the NASA Langley Unitary Plan Wind Tunnel, Test Section 2: Computational Results," AIAA Aviation (2021)



Inflow BC

$$M = 3.5, \alpha = 85^\circ, CT = 2.5$$

Momentum ρv contours at the tunnel inflow plane

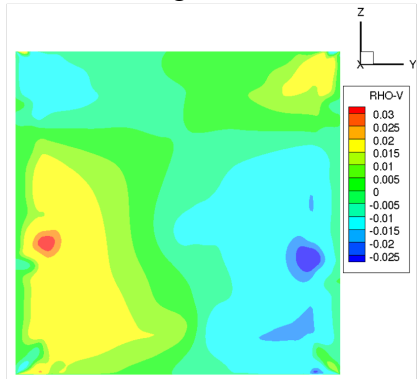


Inflow BC

$$M = 3.5, \alpha = 85^\circ, CT = 2.5$$

Momentum ρv contours at the tunnel inflow plane

Original BCs



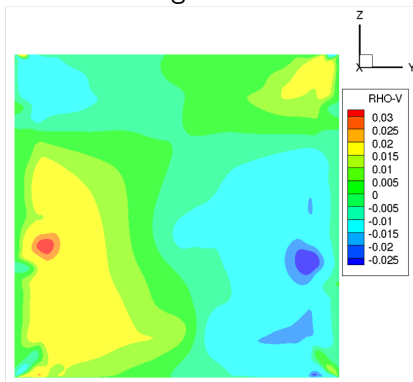


Inflow BC

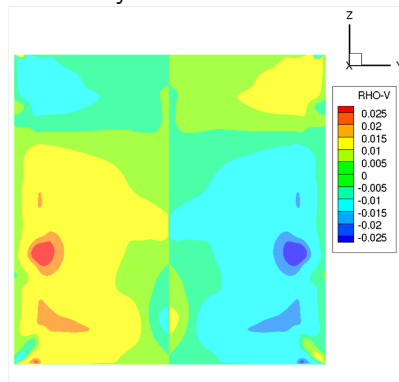
$$M = 3.5, \alpha = 85^\circ, CT = 2.5$$

Momentum ρv contours at the tunnel inflow plane

Original BCs



Symmetrized BCs

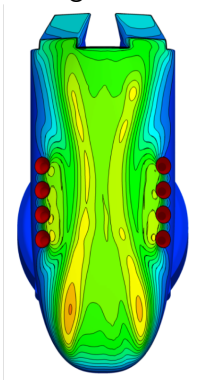




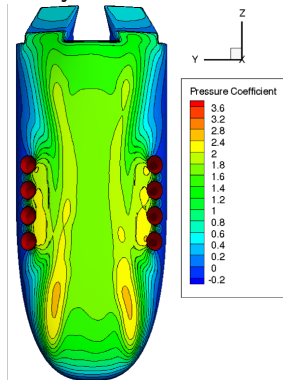
Inflow BC

$M = 3.5, \alpha = 85^\circ, CT = 2.5$
Averaged heatshield C_p contours

Original BCs



Symmetrized BCs

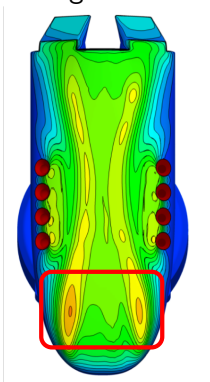




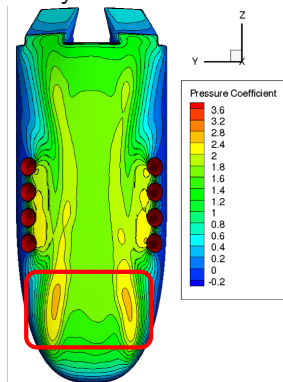
Inflow BC

$M = 3.5, \alpha = 85^\circ, CT = 2.5$
Averaged heatshield C_p contours

Original BCs



Symmetrized BCs





Turbulence Modeling



Turbulence Modeling

- SST $k - \omega$ unsteady RANS (URANS) compared to detached eddy simulation (DES)



Turbulence Modeling

- SST $k - \omega$ unsteady RANS (URANS) compared to detached eddy simulation (DES)
- Differences in load prominent for higher CT cases



Turbulence Modeling

- SST $k - \omega$ unsteady RANS (URANS) compared to detached eddy simulation (DES)
- Differences in load prominent for higher CT cases
- $M = 2.4, \alpha = 90^\circ, CT = 2.5$

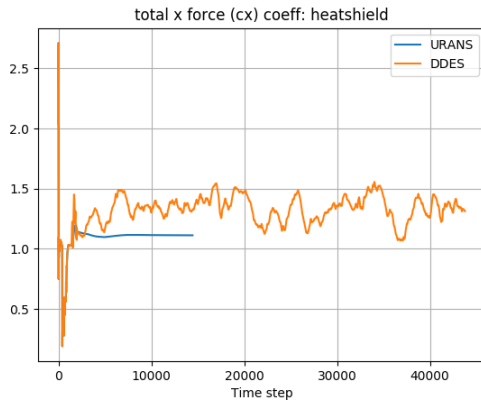


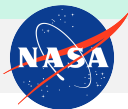
Turbulence Modeling

$$M = 2.4, \alpha = 90^\circ, CT = 2.5$$

DES raises the heatshield c_x by about 20% and greatly increases load unsteadiness compared to URANS

	c_x mean	c_x std. dev.
URANS	1.113	7.9×10^{-3}
DES	1.334	1.01×10^{-1}



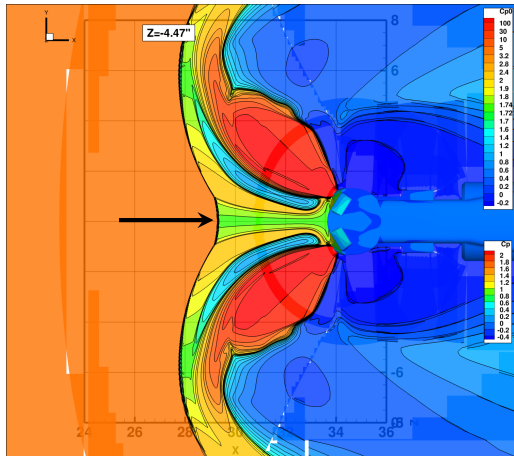


Turbulence Modeling

$$M = 2.4, \alpha = 90^\circ, CT = 2.5$$

Contours of stagnation pressure coefficient C_{p0}

SST $k - \omega$ URANS



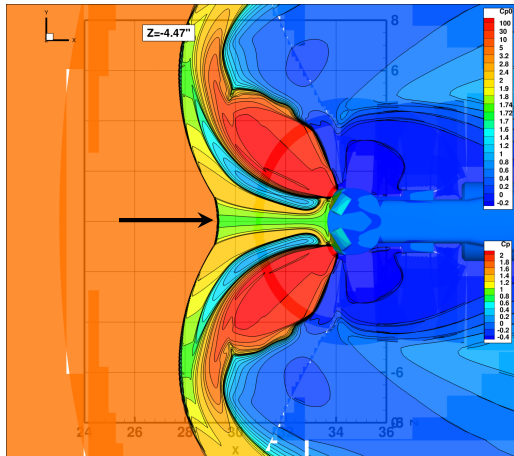


Turbulence Modeling

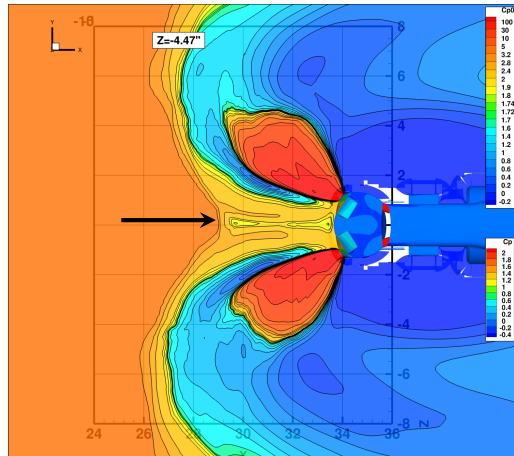
$$M = 2.4, \alpha = 90^\circ, CT = 2.5$$

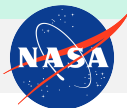
Contours of stagnation pressure coefficient C_{p0}

SST $k - \omega$ URANS



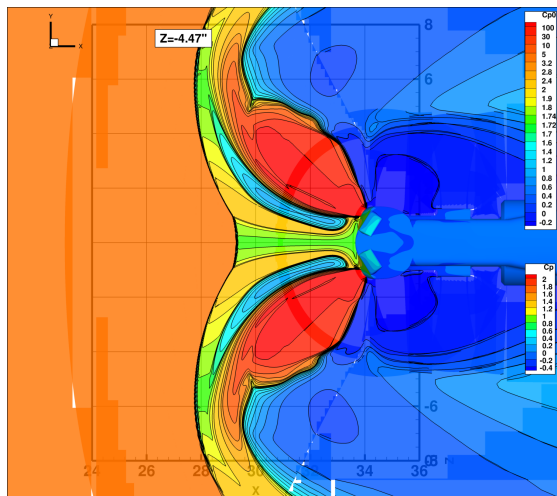
SST $k - \omega$ DES





Summary

- Present CobraMRV pre-test solutions are independent of time stepping and mesh adaption frequency
- Dynamic AMR must be used to capture the full range of vehicle dynamics
- Inflow asymmetry impacts vehicle loads
- SST $k - \omega$: DES gives 20% increase in loads compared to URANS



Acknowledgements: Funding provided by AETC DSS and NESC LAV projects.
 Contact: kristen.v.matsuno@nasa.gov

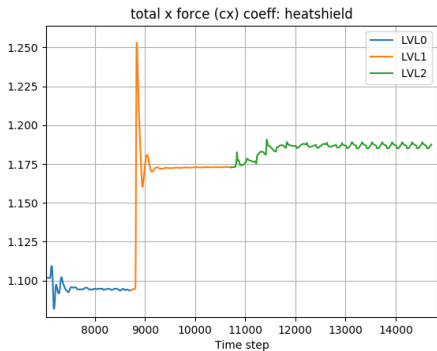


Numerical methods

- 5th order WENO
- HLLC++ in shock region, HLLC elsewhere
- ‘time-accurate’ mode
- Two levels of AMR in shock and plume regions
- Inflow conditions: averaged ‘empty tunnel’ solutions (Childs et al. AIAA Aviation (2021))
- Base turbulence model: SST $k - \omega$
 - QCR on in tunnel wall grids; disabled elsewhere
 - RC on
 - CC off

$M = 2.4, \alpha = 90^\circ, CT = 0.5$

Heatshield loads at each AMR level





Misc. Notes

- Due to unsteadiness and scale resolution, DES is likely (at least) an order of magnitude more expensive than URANS
- Nozzle boundary conditions: P_0, T_0 specified, then run with multigridding through transient period